Pipes, Paper presented at the Symposium on Two-Phase Flow, Exeter, 21-23 June, 1965, Paper C3 (1965).
Hughmark, G. A., "Film Thickness, Entrainment, and Pressure Drop in Upward Annular and Dispersed Flow," *AIChE J.*, **19**, 1062 (1973).
Kays, W. M., *ASME Paper 71-HT-44* (1970).
Levy, S., "Prediction of Two-Phase Annular Flow with Liquid Entrainment," *Intern. J. Heat Mass Trans.*, **9**, 171 (1966).
Miya, M., "Properties of Roll Waves," Ph.D. thesis, Univ. Ill., Urbana (1970).
Schlichting, H., *Boundary-Layer Theory*, McGraw-Hill, New York (1968).
Semenov, P. A., *Zh. Tekhn. Fiz.*, **14**, 427 (1944).
Shearer, C. J., and R. M. Nedderman, "Pressure Gradient and Liquid Film Thickness of Gas/Liquid Mixtures: Application to Film Cooler design," *Chem. Eng. Sci.*, **20**, 671 (1965).
Swanson, R. W., "Characteristics of the Gas-Liquid Interface in Two-Phase Annular Flow," Ph.D. thesis, Univ. Del., Newark (1966).
Wallis, G. B., *One-Dimensional Two-Phase Flow*, McGraw-Hill, New York (1969).
Webb, D., "Studies of the Characteristics of Downward Annular Two-Phase Flow," *AERE—R 6426* (1970).
Whalley, P. B., G. F. Hewitt, and P. Hutchinson, "Experimental Wave and Entrainment Measurements in Vertical Annular Two-Phase Flow," *AERE—R 7521* (1973).
Willis, J. J., "Upwards Annular Two-Phase Air/Water Flow in Vertical Tubes," *Chem. Eng. Sci.*, **20**, 895 (1965).
Wright, D., and D. Laufenbrenner, Chem. E. 379 Course Report (1975).

Manuscript received March 12, 1976; revision received August 20, and accepted August 31, 1976.

Mass Transfer of Dissolved Gases Through Tubular Membrane

THOMAS E. TANG
and
SUN-TAK HWANG
Division of Materials Engineering
The University of Iowa
Iowa City, Iowa 52242

Mass transfer characteristics are studied theoretically and experimentally for dissolved oxygen and carbon dioxide in fully developed laminar flow through a gas permeable membrane tubing. The gas transfer rate is correlated with the liquid flow rate and tubing size. Membrane resistance together with liquid phase resistance determine the overall mass transport rate.

SCOPE

In recent years, polymer membranes have been employed in industry as media for the separation or purification of mixtures which are otherwise difficult to separate economically (Lacey and Loeb, 1972; Hwang and Kammermeyer, 1975). Membrane processes such as dialysis, electrodialysis, reverse osmosis, and gas separation are often limited by slow solute transport in the liquid phase.

Liquid phase resistance to dissolved gas permeation was not recognized in earlier work (Yasuda, 1967). Later, the importance of liquid boundary resistance was reported by Hwang et al. (1971) in their study of the effect of membrane thickness on permeability. Recently, however, liquid resistance has been considered as the rate controlling resistance, and membrane resistance is usually ignored. In this paper both membrane and liquid resistances are taken into consideration to treat the general case, and the significance of membrane phase resistance relative to the liquid phase resistance is studied. Water containing low oxygen or high carbon dioxide content was passed through silicone rubber membrane tubing. Oxygen in the atmosphere permeates through the membrane into water, and the dissolved carbon dioxide permeates back into the atmosphere. The dissolved gas concentration and wall flux vary along the tube length. This boundary condition differs from the common assumption of constant concentration or constant wall flux.

The solution to this problem reveals the significance of membrane resistance to the gas transfer under various operating conditions. It provides information as to when membrane resistance can and cannot be neglected. The results developed in this paper can be applied to predict the performance of other membrane processes and to evaluate transport parameters, such as membrane permeability and solute diffusivity.

CONCLUSIONS AND SIGNIFICANCE

Permeation rates of dissolved oxygen and carbon dioxide in laminar water flow are measured under various experimental conditions. The theoretical concentration profile of dissolved gas is obtained by numerical solution for a general case, in which membrane resistance is not negligible compared with the liquid phase resistance. The changes in cup mixing concentration are correlated with the dimensionless tube length X and the system parameter E. The agreement between theoretical values and experimental data is shown to be satisfactory for many different experimental conditions. The upper bound is calculated for the change of cup mixing concentration by neglecting membrane resistance. It is found that the membrane resistance becomes a significant part of the overall resistance to the dissolved gas permeation when $E < 30$ and/or $X < 0.01$. For practical application and convenience, a performance coefficient ϕ is defined as flux per unit initial pressure gradient, which can be theoretically calculated. A good agreement is achieved between the theory and experimental results.

Thomas E. Tang is with Dalton Research Center, University of Missouri, Columbia, Missouri 65201.

The present analysis may be generalized to be applicable to any tubular membranes, fluid flow, and permeating gases. It provides the fundamental information for the analysis and design of dissolved gas permeation systems. Especially, it will be useful for the design and operation of a tubular membrane oxygenator.

PREVIOUS WORK

The study of dissolved gas permeation has been motivated by its application in the membrane oxygenator. Unlike gas phase permeation, the transfer of dissolved gases involves the resistance of a liquid phase. The first quantitative report on dissolved gas permeation was given by Robb (1965). He demonstrated that dissolved oxygen would permeate from water into a submerged cage covered by a thin silicone rubber membrane in amounts adequate to sustain life in test animals for several days. This dissolved oxygen permeation appeared to be a liquid-membrane-gas process. The permeability of dissolved oxygen in this system was lower than that of a gas-membrane-gas system, and the presence of a water boundary layer next to the membrane surface was suggested to be the cause. Yasuda (1967) presented a comparison of oxygen permeability in liquid-membrane-liquid transport with that in gas-membrane-gas transport. Oxygen permeability coefficients of several plastic membranes were compared. The data revealed that for silicone rubber and polyethylene membranes, permeability coefficients in the liquid-membrane-liquid transport system were much smaller than those in the gas-membrane-gas transport system. The lower oxygen permeability in the former system was attributed to concentration polarization at the interfaces of membrane and water. Tang (1969) and Hwang et al (1971) also investigated the liquid-membrane-liquid permeation of dissolved oxygen through silicone rubber membrane sheets. The apparent oxygen permeability increased with increasing membrane thickness and asymptotically approached the gas phase permeability. A general equation was developed to explain this phenomenon based on the concept of immobile boundary layers. Hwang and Strong (1973) continued the study using carbon dioxide and silicone rubber. They observed a similar phenomenon.

THEORY

When liquid containing low oxygen and/or high carbon dioxide content flows through membrane tubing, oxygen and/or carbon dioxide will exchange through the membrane with gases in the atmosphere owing to the partial pressure driving forces. Finally, at steady state, partial pressure profiles of the gases are developed. Material balance for the dissolved oxygen or carbon dioxide yields

$$\nabla \cdot \vec{J} = \frac{1}{r}\frac{\partial}{\partial r}(rJ_r) + \frac{1}{r}\frac{\partial J_\theta}{\partial \theta} + \frac{\partial J_x}{\partial x} = 0 \qquad (1)$$

If the following assumptions are made for a fully developed laminar flow

1. $J_\theta = 0$
2. $J_x = J_x(r, x) = C(r, x)v_x(r)$, that is, J_x due to convection only and
3. $J_r(r, x) = -D_L\, \partial C/\partial r$, that is, J_r due to diffusion only, then Equation (1) becomes

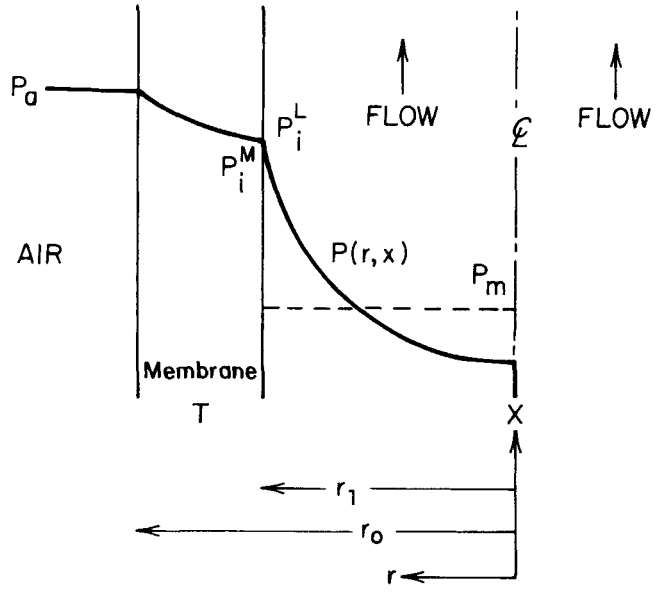

Fig. 1. Schematic plot of partial pressure profile of dissolved gas with negligible interfacial resistance.

$$\frac{1}{r}\frac{\partial}{\partial r}\left(-D_L r\frac{\partial C}{\partial r}\right) + v_x(r)\frac{\partial C}{\partial x} = 0 \qquad (2)$$

or

$$D_L\frac{\partial^2 P}{\partial r^2} + \frac{D_L}{r}\frac{\partial P}{\partial r} = v_x\frac{\partial P}{\partial x} \qquad (3)$$

where

$$D_L = \text{constant}, \quad C = S_L P$$

and

$$v_x = v_x(r) = 2v_m[1 - (r/r_i)^2]$$

For tubular flow with a fully developed velocity profile and uniform dissolved gas concentration at the point where gas exchange begins, the following two boundary conditions apply:

B.C. 1. $P = P_o = \text{constant at } x = 0$

B.C. 2. $\partial P/\partial r = 0 \text{ at } r = 0$

The third boundary condition is the continuity of mass flux at the membrane-liquid interface. If interfacial resistances to gas transfer are neglected, the partial pressure profile can be represented by Figure 1. The flux at the membrane-liquid interface, that is, $r = r_i$, is

$$J^l = -D_L\frac{\partial C^L}{\partial r}\bigg|_{r=r_i} = -D_M\frac{C_a^M - C^M(r_i, x)}{r_i \ln(r_o/r_i)} \qquad (4)$$

where

$$C^L = S_L P; \quad C^M = S_M P$$

or

$$-D_L S_L\frac{\partial P}{\partial r}\bigg|_{r=r_i} = -D_M S_M\frac{P_a - P_i^L}{r_i \ln(r_o/r_i)}$$

where

$$P_i^L = P_i^M$$

that is

B.C. 3.

$$\frac{\partial P}{\partial r} = \frac{D_M S_M (P_a - P_i^L)}{D_L S_L r_i \ln(r_o/r_i)} \quad \text{at} \quad r = r_i \tag{5}$$

If one defines

$$U = \frac{P_a - P}{P_a - P_o}$$

$$R = \frac{r}{r_i}$$

$$X = \frac{x}{ReScr_i} = \frac{\pi D_L x}{2v}$$

where

$$Re = \frac{Dv_m\rho}{\mu}; \quad Sc = \frac{\mu}{\rho D_L}$$

then Equation (3) and boundary conditions become

$$\frac{\partial^2 U}{\partial R^2} + \frac{1}{R}\frac{\partial U}{\partial R} = (1 - R^2)\frac{\partial U}{\partial X} \tag{6}$$

B.C. 1. $U = 1, \quad X = 0$

B.C. 2. $\partial U/\partial R = 0, \quad R = 0$

B.C. 3. $\partial U/\partial R = -EU, \quad R = 1$

where

$$E \equiv \frac{D_M S_M}{D_L S_L}\frac{1}{\ln(r_o/r_i)} \tag{7}$$

A numerical method can be employed to solve Equation (6). A second-order corrected finite-difference analogue, the Crank-Nicolson method (Rosenberg, 1969), is used here:

$$\left.\frac{\partial^2 U}{\partial R^2}\right|_{m,n+1/2} = \frac{1}{2}\left(\frac{U_{m+1,n+1} - 2U_{m,n+1} + U_{m-1,n+1}}{h^2} + \frac{U_{m+1,n} - 2U_{m,n} + U_{m-1,n}}{h^2}\right)$$

$$\left.\frac{1}{R}\frac{\partial U}{\partial R}\right|_{m,n+1/2} = \frac{1}{2R_m}\left(\frac{U_{m+1,n+1} - U_{m-1,n+1}}{2h} + \frac{U_{m+1,n} - U_{m-1,n}}{2h}\right)$$

$$\left.(1 - R^2)\frac{\partial U}{\partial X}\right|_{m,n+1/2} = (1 - R_m^2)\left(\frac{U_{m,n+1} - U_{m,n}}{2(k/2)}\right)$$

where h and k are mesh sizes in R and X, respectively. The Crank-Nicolson equation is the result of successive applications of the forward and backward difference equations. It is stable for all values of the ratio h/k. After derivatives are replaced with difference analogues, Equation (6) becomes

$$A_m U_{m-1,n+1} + B_m U_{m,n+1} + C_m U_{m+1,n+1} = D_m, \quad 2 \le m \le M - 1 \tag{8}$$

where

$$A_m = \frac{1}{2h^2} - \frac{1}{4R_m h}$$

$$B_m = -\frac{1}{h^2} - (1 - R_m^2)\frac{1}{k}$$

$$C_m = \frac{1}{2h^2} + \frac{1}{4R_m h}$$

$$D_m = \left(\frac{1}{4R_m h} - \frac{1}{2h^2}\right)U_{m-1,n} + \left(\frac{1}{h^2} - \frac{1 - R_m^2}{k}\right)U_{m,n} - \left(\frac{1}{2h^2} + \frac{1}{4R_m h}\right)U_{m+1,n}$$

Equation (8) contains three unknowns: $U_{m-1,n+1}$, $U_{m,n+1}$, and $U_{m+1,n+1}$. The finite-difference analogues of B.C. 2 and 3 are

B.C. 2.

$$B_1 U_{1,n+1} + C_1 U_{1,n+1} = D_1 \tag{9}$$

where

$$B_1 = 1/k + 2/h^2$$

$$C_1 = -2/h^2$$

$$D_1 = (1/k - 2/h^2)U_{1,n} + (2/h^2)U_{2,n}$$

B.C. 3.

$$A_M U_{M-1,n+1} + B_M U_{M,n+1} = D_M \tag{10}$$

where

$$A_M = -1.0$$

$$B_M = 1 + Eh + Eh^2/2$$

$$D_M = 0$$

Equations (8), (9), and (10) constitute a set of $M + 1$ algebraic equations with $M + 1$ unknowns.

By using a known feed condition, that is

B.C. 1: $U_{m,1} = 1 \quad \text{at } X = 0$

the above set of equations can be solved to yield $U_{1,2}$, $U_{2,2}$, $U_{3,2}$, . . ., $U_{M,2}$. These values in turn are used to calculate $U_{1,3}$, $U_{2,3}$, . . ., $U_{M,3}$. This system of simultaneous equations can be represented by a tridiagonal coefficient matrix and can be solved most efficiently by the method of Thomas (Rosenberg, 1969*b*).

The algorithm of the method is first to compute

$$\beta_m = B_m - A_m C_{m-1}/\beta_{m-1} \quad \text{with} \quad \beta_1 = B_1$$

$$\gamma_m = \frac{D_m - A_m\gamma_{m-1}}{\beta_m} \quad \text{with} \quad \gamma_1 = \frac{D_1}{B_1}$$

The values of the U's are then computed backwards from U_M to U_1:

$$U_{M,n+1} = \gamma_M$$

$$U_{m,n+1} = \gamma_m - \frac{C_m U_{m+1,n+1}}{\beta_m}$$

A normalized partial pressure change can be defined as $\theta = (P - P_o)/(P_a - P_o) = 1 - U$. Once the partial pressure profile is known, the cup mixing partial pressure θ_m and the average flux J can be evaluated:

$$U_m \equiv \frac{\int_0^1 Uv(R)RdR}{\int_0^1 v(R)RdR} \quad \text{where} \quad v(R) = 2v_m(1 - R^2)$$

$$= 4\int_0^1 U(R - R^3)dR \tag{11}$$

$$\theta_m = \frac{P_m - P_o}{P_a - P_o} = 1 - U_m$$

$$J = -\frac{V(P_m - P_o)S_L}{\pi DL} = -\frac{V(1 - U_m)(P_a - P_o)S_L}{\pi DL} \tag{12}$$

Table 1. The Averages of Literature Data on Solubility S_L, Diffusivity D_L in Water, and Permeability Q_M Through Silicone Rubber at 25°C

Gas	$D_L \times 10^5$ (cm^2/s)	$S_L \times 10^2$ $\left(\frac{\text{std. cm}^3}{\text{cm}^3 \cdot \text{bar}}\right)$	$Q_M \times 10^6$ $\left(\frac{\text{std. cm}^3 \cdot \text{cm}}{\text{cm}^2\ \text{s bar}}\right)$
Oxygen	2.1	2.78	4.50 (6.0×10^{-8})*
Carbon dioxide	1.9	75.0	22.5 (30×10^{-8})*

From Tang (1975).

* The quantities in parentheses are given in the more popular unit of (std. cm^3) (cm)/(cm^2) (s) (cm Hg).

Upper Bound Solution

It will be very useful if a theoretical upper bound of θ_m can be calculated. The gas transfer rate and θ_m get higher when the membrane resistance becomes smaller. An upper bound of θ_m is reached if the membrane resistance is neglected. Then B.C. 3 for Equation (6) becomes

B.C. 3. $U = 0$, at $R = 1$

This is the classic Graetz problem in heat transfer of fluid in a pipe at constant wall temperature (Jacob, 1949), if U is considered to be the dimensionless temperature of the fluid. Graetz solved the problem in the form of an infinite series:

$$U^u(X, R) = \sum_{n=1}^{\infty} C_n R_n(R) \exp(-\lambda_n^2 X) \qquad (13)$$

However, he only evaluated the first three terms. Sellars et al. (1956) and Kays (1966) reevaluated the eigenvalues and eigenfunctions. Kays' results are employed in the calculation of this study.

EXPERIMENTAL METHOD

Deaerated or carbon dioxide enriched water was allowed to flow through silione rubber membrane tubing (SILASTIC, Dow Corning). Deaerated water was prepared by boiling distilled water to expel dissolved gases. Carbon dioxide enriched water was obtained by bubbling pure carbon dioxide through deaerated water. The carbon dioxide partial pressure was kept at the level of 9.0 cm Hg (0.12 bar). A 2.5 gal stainless steel tank equipped with an O ring sealed lid was used as a water reservoir. A sufficiently long piece of thin wall glass tubing was inserted to assure a fully developed velocity profile in the silicone rubber section (Langhaar, 1942). Thus, the entrance effect could be safely neglected. Flow rates were monitored by an RGI floating-ball flowmeter and were measured again at the outlet by a volumetric flask and a stopwatch. Since the flow was induced by a hydrostatic head, a constant flow rate could be maintained. All experiments were carried out at room temperature (25° ± 3°C). A Beckman Oxygen Analyzer, Model 777, was used to measure the partial pressure of dissolved oxygen in the water, and an IL model 113-S2 Blood pH/Gas Analyzer was employed for dissolved carbon dioxide. The oxygen or carbon dioxide probe was housed in a 5 cm^3 mixing chamber. It was connected between the outlet of the membrane tubing and the flowmeter. Therefore, only the cup mixing average values could be measured for the partial pressures of dissolved gases. The experiments were conducted for the three sizes of membrane tubings (0.147, 0.455, and 0.892 cm I.D.) with various lengths (76 to 469 cm) and flow rates (2.7 to 153 cm^3/min).

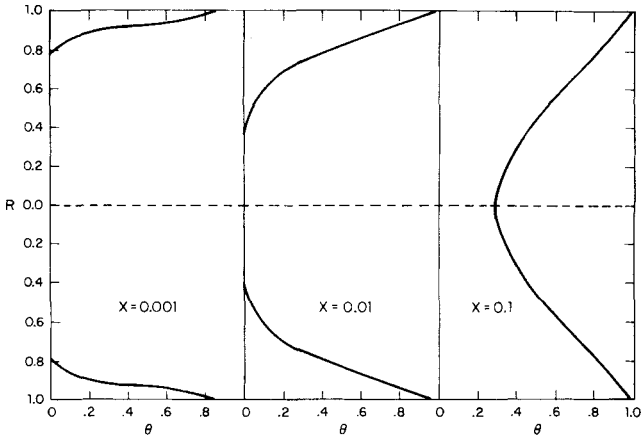

Fig. 2. Theoretical partial pressure profile for a tube of $r_i = 0.227$ cm and $r_0 = 0.264$ cm.

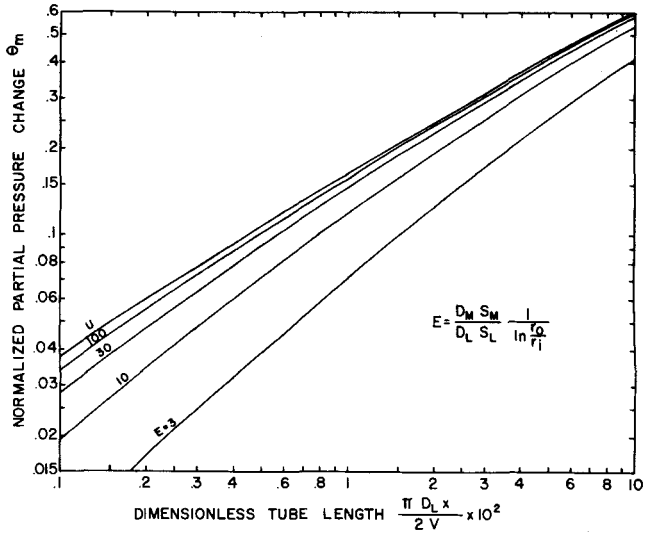

Fig. 3. Theoretical curves of cup-mixing partial pressure change.

RESULTS AND DISCUSSION

In the numerical calculations, various grid sizes were tried ranging from 0.1 to 0.005 for R and from 0.01 to 0.00001 for X. It was found that convergence of the numerical solution was satisfactory for grid size 0.025 for R and 0.0001 for X. This grid size was used for all calculations throughout the study. A typical example is given in Figure 2 for the calculated profile of dissolved oxygen partial pressure for a tube of 0.455 cm I.D. and 0.0371 cm wall thickness. The theoretical values of cup-mixing pressure θ_m are plotted against X for four E values in Figure 3. The average values (Tang, 1975) of literature data on solubility S_L, diffusivity D_L, and permeability Q_M in Table 1 were used in the calculations. The experimental results of θ_m are plotted against X in Figure 4, 5, 6, and 7 for the three tube sizes. The plots show that experimental results of θ_m agree fairly well with the theoretical values.

Since the normalized pressure change of the experimental data agrees quite well with theoretical values, Figure 3 can be used for general application. It can be applied to any membrane tubing, any fluid flow, and any permeating gas as long as the basic assumptions and boundary conditions mentioned in the theory section are satisfied. The system parameter E can be rewritten in the form

$$E = \frac{Q_M}{Q_L} \frac{1}{\ln(1 + T^*)} \qquad (14)$$

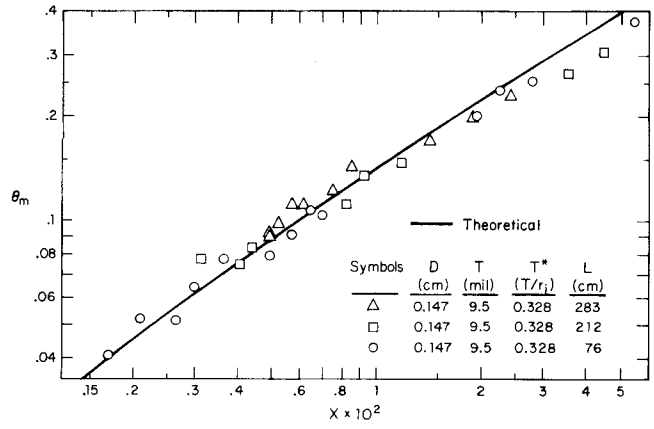

Fig. 4. Correlation of θ_m with X for oxygen absorption, $E = 27.2$.

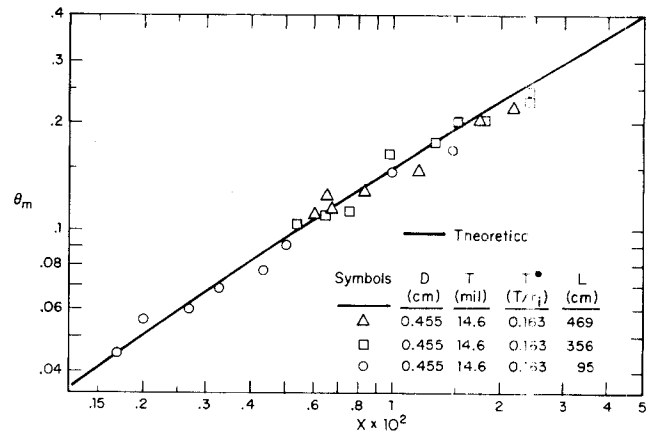

Fig. 5. Correlation of θ_m with X for oxygen absorption, $E = 51.1$.

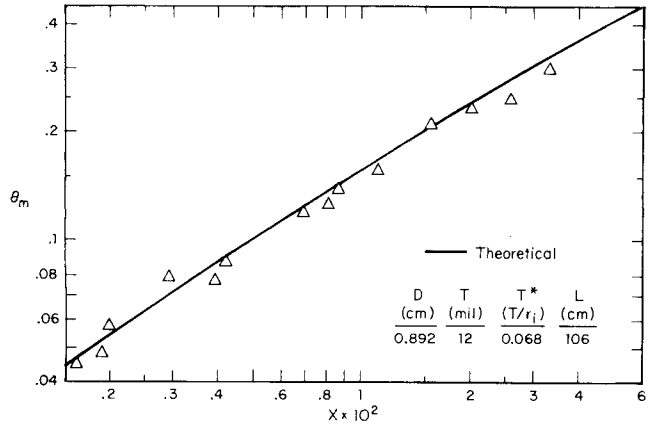

Fig. 6. Correlation of θ_m with X for oxygen absorption, $E = 117$.

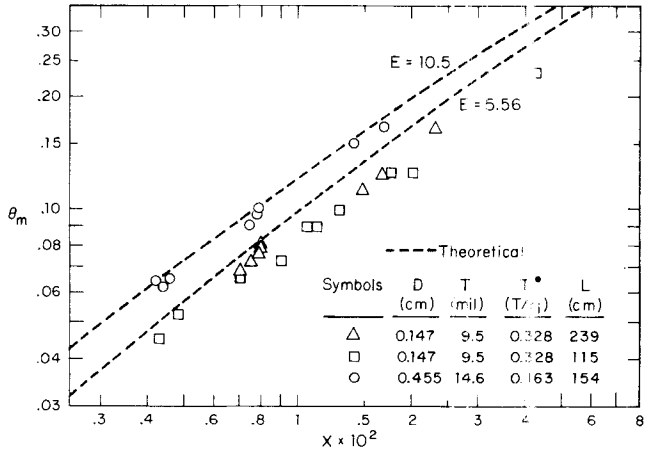

Fig. 7. Correlation of θ_m with X for carbon dioxide removal.

Q_L is defined as the permeability of stagnant liquid film. Thus E is a function of the ratio of the membrane permeability to the liquid film permeability and the normalized membrane wall thickness. Also, E can be reexpressed as

$$E = \frac{D_M S_M}{r_i \ln(r_o/r_i)} \frac{r_i}{D_L S_L} = \frac{1}{R_M} \frac{r_i}{Q_L} \qquad (15)$$

where membrane resistance R_M is defined as $R_M \equiv r_i \ln(r_o/r_i)/D_M S_M$. From Equation (14) one can realize that E is fixed once the permeation system; namely, membrane, tubing size, gas, and liquid are chosen. So E is referred to as a system parameter.

Now with a better understanding of E and X, one can examine Figure 3 more closely. As shown in the figure, all curves approach curve U (upper bound) asymptotically as E increases. This becomes apparent when one examines Equation (15). Curve U is obtained by neglecting R_M, and as R_M approaches to zero, E approaches to infinity. So curve U is the asymptote. The discrepancy between a curve and the asymptote is, thus, a measure of the significance of the membrane resistance. At most operating conditions, it is appreciable to the total resistance. The error caused by neglecting the membrane resistance, however, becomes less than 10% when $E > 30$ and/or $X > 0.01$.

One can view Equation (14) from another angle. E approaches infinity as T^* approaches zero. That is, θ_m vs. X curve approaches curve U as the membrane gets thinner. Also, once the tube dimension is fixed, that is, T^* is fixed, E is directly proportional to Q_M/Q_L. So E is a measure of the relative significance of the liquid resistance to the gas permeation, which depends on liquid properties and tube dimensions as well as the properties of the membrane itself.

For silicone rubber, membrane permeability Q_M of carbon dioxide is five times that of oxygen, and for water, liquid phase permeability Q_L of carbon dioxide is 24.5 times that of oxygen. But, as shown in Figure 3, the partial pressure changes θ_m for carbon dioxide are always lower than (about one half) those for oxygen at the same X values. This is because θ_m is a function of E which depends on the ratio of Q_M to Q_L. For the same size of tubing, E value for carbon dioxide is always lower than that of oxygen, since the ratio of Q_M/Q_L value is 1:4.89 [Equation (14)]. So θ_m for carbon dioxide is lower than that for oxygen, since E value is smaller. But the actual mass transfer rate of carbon dioxide is much higher than that of oxygen, since the solubility ratio is 27.

Definition of Performance Coefficient for the Tubular Permeation System

Although it has been shown that the normalized oxygen pressure increase or carbon dioxide pressure decrease θ_m can be correlated with the dimensionless tube length X using E as a system parameter, θ_m is not usually utilized nor convenient for the evaluation or design of the tubular permeation system. Efficiency of the permeation system is determined by the rates of oxygen absorption and carbon dioxide elimination for a given liquid flow rate. It would be desirable if one could define a performance coefficient which is more practical and can be calculated theoretically.

When a permeation process involves a liquid phase, resistance to mass transfer of the liquid phase is as sig-

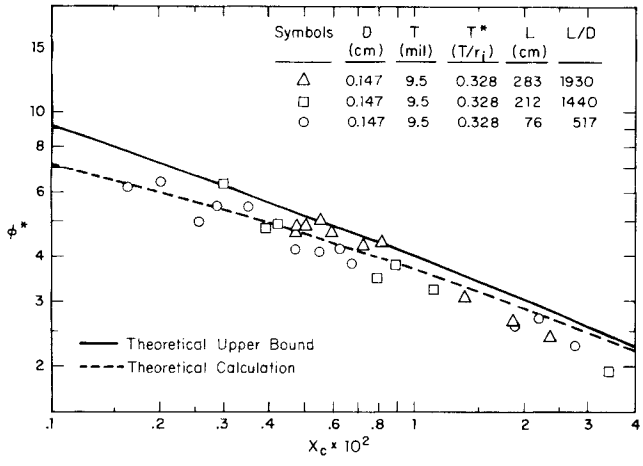

Fig. 8. Correlation of performance coefficient with X_c, $E = 27.2$.

nificant as that of the membrane phase if not greater. So the concentration gradient across both liquid phase and membrane phase should be considered in the definition of a mass transfer coefficient. In the case of tubular laminar flow, the laminar boundary layer extends to the center of the tubing. One might, therefore, define $(P_a - P_m)/r_c$ as an average local driving force, where the corrected tube radius r_c is defined as $r_c = r_i + TQ_L/Q_M$. The second term converts the tube wall thickness to an equivalent thickness of liquid layer. A performance coefficient for the tubular permeation system can be defined based on the initial driving force as

$$\phi \equiv \frac{-Jr_c}{P_a - P_o} \tag{16}$$

$$= \left(\frac{P_m - P_o}{P_a - P_o}\right) \frac{S_L V r_c}{\pi DL} = \frac{\theta_m S_L D_L}{4X_c} \tag{17}$$

where

$$X_c = \frac{1}{ReScr_c} \tag{18}$$

Here, X_c can be regarded as a corrected dimensionless tube length. Since θ_m can be theoretically calculated, ϕ can also be theoretically calculated from Equation (17). Furthermore, one can also define a dimensionless performance coefficient as

$$\phi^* \equiv \frac{\phi}{S_L D_L} = \frac{\theta_m}{4X_c} \tag{19}$$

A theoretical upper bound can be obtained by neglecting membrane resistance:

$$\phi^u = \frac{\theta_m{}^u S_L D_L}{4X_c}$$

$$\phi^{*u} = \frac{\theta_m{}^u}{4X_c} = \frac{\theta_m{}^u}{4X}$$

Theoretical and experimental values of ϕ^* together with the theoretical upper bound are plotted in Figure 8 for $D = 0.147$ cm tubing. As shown in the figure, experimental and theoretical values agree fairly well. This is also true for other tube sizes. It should be pointed out that the theoretical upper bound ϕ^{*u} was plotted against corresponding X instead of X_c, since X_c reduces to X when R_M is equal to zero. Figure 8 is a very useful plot, since ϕ^* is a function of only X_c and E explicitly. And the value E is usually fixed once the system (gas, fluid, and tube dimensions) is chosen. When X_c, which is a function of operating conditions, namely, V and L, is set, ϕ^* can be predicted directly from the plot. It is worthy of note that ϕ^* decreases as dimensionless length X increases.

The present study provides the fundamental information for the analysis and design of dissolved gas permeation systems. Both membrane resistance and liquid resistance were considered, and their contributions to the total resistance were distinguished. Gas transfer rates were correlated with the flow variables as well as the mass transfer properties of the membrane and liquid. These correlations would be particularly useful for the design and operation of a tubular membrane oxygenator.

NOTATION

A_m, B_m, C_m, D_m = coefficients in the matrix equation
C = dissolved gas concentration in membrane or liquid phase, g-mole/cm³
D = inside diameter of tubing, cm
D_L = gas diffusivity in liquid, cm²/s
D_M = gas diffusivity in membrane, cm²/s
E = system parameter defined in Equation (7)
J^l = local gas transfer flux at r_i, (std. cm³)/(s)(cm²)
J = flux at r_i averaged over tubing length, Equation (12) (std. cm³)/(s)(cm²)
L = tubing length, cm
P = gas partial pressure, bar
Q_L = gas permeability through film, $Q_L = D_L S_L$, (std. cm³)(cm)/(s)(cm²)(bar)
Q_M = gas permeability through membrane, $Q_M = D_M S_M$, (std. cm³)(cm)/(s)(cm²)(bar)
r = tubing radius, variable, cm
r_c = corrected radius, $r_c = r_i + T(Q_L/Q_M)$, cm
r_i = inside radius, $r_i = D/2$, cm
r_o = outside radius, $r_o = r_i + T$, cm
R = $R = r/r_i$
R_M = membrane phase resistance, (s)(cm²)(bar)/(std. cm³)
Re = Reynolds number
S_L = gas solubility in liquid, (std. cm³)/(cm³)(bar)
S_M = gas solubility in membrane, (std. cm³)/(cm³)(bar)
Sc = Schmidt number, $Sc \equiv \mu/\rho D_L$
T = tubing wall thickness, cm
T^* = dimensionless tubing wall thickness, $T^* = T/r_i$
U = normalized driving force, $U \equiv (P_a - P)/(P_a - P_o)$
V = volumetric liquid flow rate, cm³/s
v_x = laminar flow velocity profile, $v_x = v_x(r)$, cm/s
v_m = mean flow velocity, cm/s
x = variable for tubing length, cm
X = dimensionless tubing length, $X \equiv x/(ReScr_i)$
X_c = corrected X, $X_c \equiv X(r_i/r_c)$

Greek Letters

β, γ = parameters used in numerical calculations
θ = dimensionless pressure increase or decrease, $\theta \equiv (P - P_o)/(P_a - P_o)$
μ = viscosity, g/(s cm)
ρ = density, g/cm³
λ_n = eigenvalues defined by Equation (13)
ϕ = performance coefficient, defined by Equation (16), (std. cm³)(cm)/(s)(cm²)(bar)
ϕ^* = dimensionless performance coefficient, defined by Equation (19)

Superscripts

l = local quantity
L = liquid phase
M = membrane phase
u = upper bound

Subscripts

M, L, G = membrane, liquid, gas phase
o = at entrance
m = mean value
a = atmospheric
i = membrane-liquid interface

LITERATURE CITED

Hwang, S. T., T. E. Tang, and K. Kammermeyer, "Transport of Dissolved Oxygen through Silicone Rubber Membranes," *J. Macromol. Sci. Phys.*, **B5**, 1 (1971).

Hwang, S. T., and K. Kammermeyer, *Membranes in Separations*, p. 457, Wiley-Interscience, New York (1975).

Hwang, S. T., and G. D. Strong, "Transport of Dissolved Carbon Dioxide through Silicone Rubber Membranes," *J. Polymer Sci., Symposium No. 41*, 17 (1973).

Jacob, M., *Heat Transfer*, Vol. 1, pp. 451-461, J. Wiley, New York (1949).

Kays, W. M., *Convective Heat and Mass Transfer*, p. 128, McGraw-Hill, New York (1966).

Lacey, R. E., and S. Loeb, *Industrial Processing with Membranes*, p. 3, Wiley-Interscience, New York (1972).

Langhaar, H. L., "Steady Flow in the Transition Length of a Straight Tube," *J. Applied Mechanics, Trans. ASME*, **64**, A-55 (1942).

Robb, W. L., "Thin Silicone Membranes—Their Permeation Properties and Some Applications," *Research Lab. Bulletin*, General Electric Co., (winter 1964-1965).

Rosenberg, D., *Methods for the Numerical Solution of Partial Differential Equations*, p. 22, American Elsevier Publishing Co. New York (1969).

———, *Ibid.*, p. 113 (1969*b*).

Sellars, J. R., M. Tribus, and J. S. Klein, "Heat Transfer to Laminar Flow in a Round Tube or Flat Conduit—The Graetz Problem Extended," *Trans. ASME*, 78, 441 (1956).

Tang, T. E., "Transport of Dissolved Oxygen through Silicone Rubber Membrane," M.S. thesis, Univ. Iowa, Iowa City (1969).

———, "Mass Transfer of Dissolved Gases through Membrane Tubings," Ph.D. thesis, Univ. Iowa, Iowa City (1975).

Yasuda, H., "Basic Consideration of Permeability of Polymer Membrane to Dissolved Oxygen," *J. Polymer Sci.*, (A-1), No. 5, 2952 (1967).

Manuscript received February 2, 1976; revision received and accepted August 20, 1976.

Explaining Solubilization Kinetics

A. F. CHAN
D. FENNELL EVANS
and
E. L. CUSSLER

Department of Chemical Engineering
Carnegie-Mellon University
Pittsburgh, Pennsylvania 15213

Solubilization rates of fatty acids in pure detergent solutions are controlled by mixed micelle desorption and diffusion. Solubilization rates in partially saturated detergent solutions also involve exchange of fatty acids between the solid and the solution. These conclusions depend on models like those used in gas-solid catalysis and in tracer diffusion.

SCOPE

This paper develops and verifies theories of solubilization kinetics in aqueous detergent solutions. It includes both the physical basis of the equations and the experiments necessary to verify them. However, these systems can show chemical eccentricities which are detailed in a companion paper (Chan et al., 1976).

Except at high dilution, detergent solutions contain micelles, thermodynamically stabilized aggregates which typically are 40Å in diameter (Kratohvill and Dellicolli, 1970). These micelles, which characteristically contain about one hundred detergent molecules, have a water soluble hydrophillic surface but a water insoluble hydrophobic central core. Many smaller and larger micelles are known; for example, bile salt micelles may contain less than ten molecules (Small et al., 1969). Solubilization occurs when water insoluble molecules, that is, oils, lipids, long chain fatty acids, and the like, are incorporated into the micelles. The resulting mixed micelles retain their hydrophillic shell and their hydrophobic core.

Previous investigations of solubilization have concentrated on equilibrium studies, not kinetic ones. For example, they have contained accurate determinations of the size and charge of the mixed micelles. They have included measurements of the maximum amounts which can be solubilized by specific detergents (Elworthy et al., 1968). When these earlier studies did involve kinetics, they often used poorly defined experiments from which definite conclusions were difficult to draw.

Previous investigations of other aspects of detergent kinetics have concentrated on removal from fibers of soils of greases and particles (Jones, 1961; Schott, 1972). Once removed, the soils can be suspended in detergent solutions rather than incorporated into thermodynamically stable micelles. The studies, which were largely carried out in rapidly stirred solutions, have been explained in terms of two limiting mechanisms, a roll-up mechanism and a penetration mechanism (Schwartz, 1971). The roll-up mechanism suggested that the detergent's principal function is to alter the contact between soil and fiber; the penetration mechanisms showed that diffusion of the detergent into the soil is important. While these experiments are tremendously useful in providing a qualitative picture, they do not provide an exact description of the mass transfer rates involved in detergency. This paper presents such a description for the mass transfer rates important in one aspect of detergency, solubilization.

Correspondence concerning this paper should be addressed to E. L. Cussler.